Journal of Radioanalytical and Nuclear Chemistry (2021) 327:627–633
https://doi.org/10.1007/s10967-020-07532-8

Synthesis and evaluation of [^{99m}Tc]TcAMD3465 as a SPECT tracer for CXCR4 receptor imaging

Yitian Wu[1] · Hong Zhu[2] · Xiaojun Zhang[1] · Peng Yu[1] · Yuan Gui[3] · Zhihong Xu[3] · Jinming Zhang[1] · Jiahe Tian[1]

Received: 5 June 2020 / Accepted: 27 November 2020 / Published online: 4 January 2021

Abstract

CXCR4 plays an important role in a number of immunological-based diseases and cancers. The development of radiotracers targeting CXCR4 can provide a valuable tool for the diagnosis and monitoring of conditions involving deregulation of the receptor. The incorporation of multiple radionuclides into small molecules, peptides, and CXCR4 ligands have been reported and characterized. In this study, a ^{99m}Tc labeled AMD3465 with high yields and radiochemical purity was prepared. In vitro and in vivo study of [^{99m}Tc]TcAMD3465 showed high stability and binding affinity, with a hydrophilic log *P* value of − 2.67. Biodistribution study was investigated using tissue and organ samples with a well-type Na(I) detector, high radioactivity accumulation was observed in liver, spleen and bone, consistent with high CXCR4 expression in these organs. SPECT imaging was performed in H460 xenograft mouse model, [^{99m}Tc]TcAMD3465 showed comparable tumor uptake and a significantly high tumor-to-background ratio, suggesting potential utility of [^{99m}Tc]TcAMD3465 as a CXCR4 receptor imaging agent.

Keywords Chemokine · CXCR4 · AMD3465 · ^{99m}Tc · Tumor imaging

Introduction

The chemokine receptor (CXCR4) is a member of the CXC-chemokine family belonging to a larger superfamily of receptors known as G-protein coupled receptors (GPCRs). CXCR4 is overexpressed in a range of human cancers including breast, prostate, lung and colon cancer, as well as multiple myeloma [1–4], it also plays a role in tumor metastasis, providing an attractive target for cancer diagnosis and treatment [5, 6].

Non-invasive imaging techniques can provide a better understanding of the role of targeting biological tissues or molecules in health and disease. A lot of attempts have been made to non-invasively image CXCR4 expressing tumor, such as using SPECT or PET/CT with ^{111}In-, ^{99m}Tc-, ^{18}F-labeled peptides and ^{125}I-labeled monoclonal antibodies [7–10]. ^{68}Ga-Pentixafor, a radiolabeled cyclic pentapeptide with high affinity to CXCR4, has proven to be useful in quantification of CXCR4 [11]. A small molecule agent, AMD3100, which was the first non-peptide CXCR4 inhibitor approved for clinical use, has been labeled with ^{64}Cu, ^{67}Ga and ^{99m}Tc [12–16]. [^{64}Cu]CuAMD3100 and [^{99m}Tc]TcAMD3100 have been evaluated in healthy mice and the radioligands are accumulated in CXCR4 expressing organs such as spleen and liver. However, AMD3100 has a low affinity for CXCR4 (651 ± 37 nM), and ^{64}Cu-labeled AMD3100 showed a high non-specific liver uptake of > 40% [14]. A second-generation chelator, AMD3465 has been demonstrated to have a higher affinity, smaller molecular weight and a monocyclam structure, as well as being ten-fold more effective as a CXCR4 antagonist than AMD3100 [17, 18]. The suitability of ^{64}Cu-labeled AMD3465 for CXCR4 tumor imaging has been reported. However, significant (40%ID/g) accumulation of the labeled agent in liver has also been observed [19]. The synthesis of another PET imaging agent N-[^{11}C]methyl-AMD3465 has also been successful, the tumor-to-muscle ratio was found to be 7.85 at

✉ Jinming Zhang
zhangjm301@163.com

Hong Zhu
zh_zy@163.com

Yuan Gui
rabbitgy1981@163.com

1 Department of Nuclear Medicine, Chinese PLA General Hospital, Beijing 100853, China

2 Department of Nuclear Medicine, Nanjing General Hospital of Nanjing Command, Nanjing 21002, China

3 Huayi Isotopes, Changshu 215501, Jiangsu, China

60 min after tracer injection, and CXCR4 expression in tumors or other CXCR4 expressing tissues can be detected [20]. Nevertheless, ^{99m}Tc is widely considered the best medical radionuclide due to its favorable physical properties and reliable labeling technology, and SPECT imaging is more available and affordable compare to PET/CT. Therefore, the development of a ^{99m}Tc-based agent for AMD3465 is highly desirable and would have great potential for CXCR4 tumor imaging.

Here, we report the synthesis and ^{99m}Tc radiolabeling of AMD3465 starting from cyclam, and the detail evaluation by in vitro and in vivo studies of [^{99m}Tc]TcAMD3465 as an SPECT imaging agent for CXCR4.

Materials and methods

General

$Na^{99m}TcO_4$ was provided by the China Institute of Atomic Energy (CIAE). It was prepared by eluting from ^{99}Mo/^{99m}Tc generator in saline. All other chemicals were commercial analytical grade and used without further purification. ^{1}H-NMR spectra were recorded in $CDCl_3$ or DMSO-d_6 on a Bruker spectrometer operating at 300 MHz. Radio-TLC was performed on BioScan-2000 radio-TLC using Whatman No.1 strips.

Chemistry

Synthesis of tri-*tert*-butyl 1,4,8,11-tetraazacyclotetradecane-1,4,8-tricarboxylate (1)

The reaction was conducted as previously described [22]. Briefly, to a solution of cyclam (3.35 g, 16.7 mmol) in dichloromethane (90 mL) was added di-tert-butyl dicarbonate (9.4 g, 43.4 mmol) in dichloromethane (60 mL) slowly within 3 h at 0 °C under nitrogen. The reaction was stirred at room temperature for 12 h. Solvent was evaporated, and the crude product was purified by chromatography on silica gel eluting with gradient MeOH/DCM to give compound 1 as a white solid in 45% yield (3.8 g, 7.6 mmol). ^{1}H NMR (300 MHz, $CDCl_3$) δ 3.20–3.45 (br, 12H), 2.79 (t, 2H, J = 5.2 Hz), 2.62 (t, 2H, J = 5.2 Hz), 1.90 (br s, 2H), 1.70 (br s, 2H), 1.40–1.50 (m, 27H); LC-MS: calculated for $C_{25}H_{48}N_4O6$ 500.36; found [M + H] 501.4.

Synthesis of tri-*tert*-butyl 11-(4-(bromomethyl) benzyl)-1,4,8,11-tetraazacyclotetradecane-1,4,8-tricarboxylate (2)

The reaction was carried out according to reported procedures [22]. To a heated solution of dibromoxylene (5.25 g 19.9 mmol) in CH_3CN (30 mL) at 90 °C was added K_2CO_3 (1.00 g, 5.45 mmol), followed by a solution of compound 1 (2.4 g, 4.8 mmol) in CH_3CN (45 mL) slowly within 1.5 h. The reaction was kept at 90 °C until completion. The solvent was evaporated and the residue was purified by chromatography on silica gel eluting with gradient MeOH/DCM to give compound 2 as a white solid in 49% yield (1.6 g, 2.3 mmol). ^{1}H NMR (300 MHz, $CDCl_3$) δ 7.31 (d, J = 7.9 Hz, 2H), 7.23 (d, J = 8.0 Hz, 2H), 4.48 (s, 2H), 3.52 (s, 2H), 3.20–3.50 (m, 12H), 2.62(br s, 2H), 2.38 (br s, 2H), 1.90 (br s, 2H), 1.55–1.75 (m, 2H), 1.30–1.50 (m, 27H); LC-MS: calculated for $C_{33}H_{55}BrN_4O_6$ 682.3, 684.3; found [M + H] 683.3, 685.3.

Synthesis of tri-*tert*-butyl 11-(4-(((pyridin-2-ylmethyl) amino)methyl)benzyl)-1,4,8,11-tetraazacyclotetradecane-1,4,8-tricarboxylate (3)

K_2CO_3 (0.225 g, 1.62 mmol) was added to a solution of 2-(aminomethyl)pyridine (0.465 g, 4.3 mmol) in CH_3CN (30 mL). The suspension was heated to 80 °C, and a solution of compound 2 (0.60 g, 0.90 mmol) in CH_3CN (20 mL) was added slowly over 2 h. The reaction was refluxed for 40 min, concentrated and purified by chromatography on silica gel eluting with gradient MeOH/DCM to give compound 3 in 80% yield (0.5 g, 0.7 mmol). ^{1}H NMR (300 MHz, $CDCl_3$) δ 8.57 (d, 1H, J = 4.2 Hz), 7.66 (dt, 1H, J = 1.8,7.7 Hz), 7.16–7.35 (m, 6H), 3.99 (s,2H), 3.87 (s, 2H), 3.52 (s, 2H), 3.20–3.42 (m, 12H), 2.60 (br s, 2H), 2.38 (br s, 2H), 1.90 (br s, 2H),1,0.67 (br s, 2H), 1.30–1.50 (m, 27H); LC-MS: calculated for $C_{39}H_{62}N_6O_6$ 710.47; found [M + H] 711.5, [M + Na] 733.5.

Synthesis of *N*-(4-((1,4,8,11-tetraazacyclotetradecan-1-yl) methyl)benzyl)-1-(pyridin-2-yl)methanamine (AMD3465)

12 M HCl (10 mL) was added slowly to a solution of compound 3 (0.50 g, 0.70 mmol) in CH_3OH (15 mL). The solution was stirred at room temperature for 10 h. The methanol was evaporated and the resulting solid was washed with ether and filtered to give AMD3465 as yellow solid in 89% yield (0.37 g, 0.62 mmol). ^{1}H NMR (300 MHz, DMSO) δ 11.9 (br s, 1H), 9.60–10.4 (m, 8H), 8.64 (d, J = 4.2 Hz, 1H), 7.92 (dt, J = 1.8,7.7 Hz, 1H), 7.60–7.68 (m, 4H), 7.56(d, J = 7.9 Hz, 1H), 7.45–7.50 (m, 1H), 4.35 (br s, 2H), 4.32 (s, 2H), 4.28 (s, 2H), 3.42–3.58 (m, 8H), 3.20–3.38 (m, 8H), 2.08–2.30 (m, 4H); LC-MS: calculated for $C_{24}H_{38}N_6$ 410.32;found [M + H] 411.4.

Radiochemistry

The [^{99m}Tc]TcAMD3465 was prepared similarly to [^{99m}Tc] TcAMD3100 [12]. Briefly, an AMD3465 solution was prepared by dissolving 0.1 mg AMD3465 in 0.5 mL H_2O

and the pH was adjusted to 7.0 using 1 mol/L citrate solution. Then freshly prepared $SnCl_2$ solution (300 µL; 1 mg $SnCl_2$/1 mL H_2O) was added followed by 1850 MBq (50 mCi) of $Na^{99m}TcO_4^-$. The mixture was kept at ambient temperature for 20 min to give [^{99m}Tc]TcAMD3465. Formation of the labeled compound was confirmed by radio-TLC analysis. Approximately 2 µL [^{99m}Tc]TcAMD3564 was spotted on Whatman No. 1 paper strips. The strips were developed by two different solvents: acetone and saline. With saline as the eluent, the hydrated $^{99m}TcO_2$ impurities remained at the original point, while [^{99m}Tc]TcAMD3465 and the free $^{99m}TcO_4^-$ migrated to the solvent front. With acetone as the eluent, [^{99m}Tc]TcAMD3465 and the hydrated $^{99m}TcO_2$ remained at the original point, while the free $^{99m}TcO_4^-$ migrated with the solvent. When the solvent reached the desired distance, the strips were taken out and the radioactivity was scanned on AR2000.

Measurement of partition coefficient

Octanol-water partition coefficient was determined by measuring the distribution of [^{99m}Tc]TcAMD3465 in n-octanol and 0.01 mol/L PB (pH 7.4). A sample of [^{99m}Tc]TcAMD3465 (100 µL) was diluted with PB (900 µL), and was mixed with n-octanol (1 mL). The mixture was vortexed for 5 min, and then centrifuged at 4000 rpm for 5 min to ensure separation of two layers. 10 µL aliquots were collected from both layers and each radioactivity was counted with counter respectively. Log *P* value was calculated using Log *P* = log(CPM for octanol/CPM for water) and is reported as the average of three independent experiments.

In vitro stability study

The in vitro stability of [^{99m}Tc]TcAMD3465 was studied by measuring radiochemical purity (RCP) in 0.01 mol/L NaH_2PO_4 buffer (PB) and 1% BSA at different time intervals (1, 2, 4, 8 and 24 h) at room temperature using radio-TLC.

In vitro receptor binding assays

The in vitro receptor binding assays were performed on Jurkat-T cells to test the binding affinity in homologous competition as described elsewhere [13]. Briefly, Jurkat-T cells were harvested and seeded in 12-well plates at a density of 10^5 cells per well. After 24 h, the cells were washed two times with 0.5 mL PBS. The cells were treated with unlabeled AMD3465 solution at the final concentration of 10^{-6} to 10^{-3} M, following by incubation with 100 nmol/L of [^{99m}Tc]TcAMD3465. Cells were incubated in 1000 µL binding buffer (PBS containing 5 nM $MgCl_2$, 1 nM $CaCl_2$, 0.25% BSA) at 37 °C for 1 h. After incubation, cells were washed twice with 0.5 mL cold binding buffer. The uptake of cells was counted and the IC_{50} values were determined by nonlinear regression analysis using GraphPad Prism 5.0 and reported as mean of triplicate measurements.

Tumor models

Animal experiments were conducted under a protocol approved by the PLA Animal Care and Use Committee. All work was performed in accordance with the terms of the Animals (Scientific Procedures) Act 1986, Regulations of Beijing Municipality on the administration of experimental animals 2004, Guiding opinions on treating animals well 2006 and Guidelines for ethical review of laboratory animal welfare in Beijing. Providing a clean, comfortable and safe living environment for experimental animals, and give them enough feed and clean water. During the use of animals, panic and pain should be minimized. Female nude mice obtained from Academy of Military Medical Sciences at 6 weeks of age were injected subcutaneously in the right hind leg with 10^7 H460 lung adenocarcinoma cells. When the tumors reached 1.0 cm in diameter, the mice were used for SPECT imaging.

Biodistribution studies

A dose of 3.7 MBq [^{99m}Tc]TcAMD3465 was injected through the tail vein into five groups of normal NH mice (20–22 g, n = 5/group). The mice were sacrificed at 30 min, 60 min, and 90 min post injection and the organs of interest (blood, heart, liver, spleen, lung, kidneys and others) were dissected and weighed, the uptake of each organ was counted by a well-type Na(I) detector and expressed as the percentage of injection dose per gram (%ID/g). All biodistribution studies were carried out in compliance with the national laws related to the conduct of animal experimentation.

SPECT imaging

The SPECT imaging was performed in both normal NH mice and tumor bearing mice. [^{99m}Tc]TcAMD3465 was injected to mice via the tail vein at a dose of 15 MBq in 0.2 mL PBS. The mice were anesthetized with isoflurane/O_2. The whole body imaging was performed using Siemens SPECT with pinhole collimator at 60 min after injection.

Results

Chemistry and radiolabeling

AMD3465 was synthesized by a four-step reaction sequence starting from cyclam (Scheme 1). The intermediates and the target compound were characterized by ^{1}H-NMR and

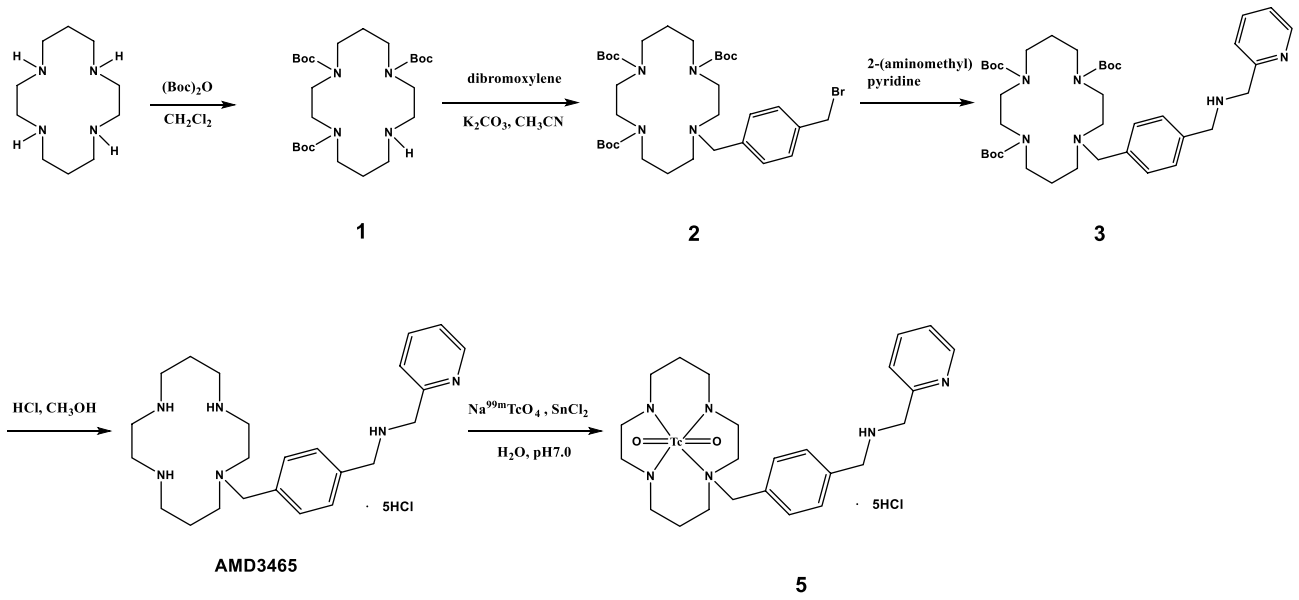

Scheme 1 Synthesis of AMD3465 and ^{99m}Tc-AMD3465

mass spectrometry, with the results conforming to expected chemical structures. AMD3465 was labeled with $Na^{99m}TcO_4$ by reduction with stannous chloride. For thin layer chromatography (TLC) analysis, a two-eluent system (acetone and saline) similar to that for [^{99m}Tc]TcAMD3100 was used. It was found that the radiochemical purities (RCP) of [^{99m}Tc]TcAMD3465 were greater than 99% (Fig. 1), and the specific activity was > 37 GBq/μmol. The radiolabeled compound was used directly for in vitro and in vivo studies.

1. Synthesis of AMD3465 and [^{99m}Tc]TcAMD3465.

Measurement of partition co-efficient

The partition co-efficient (log *P*) value of [^{99m}Tc]TcAMD3465 was determined to be − 2.67, similar to the log *P* of − 2.71 reported for [^{64}Cu]CuAMD3465 [19], suggesting a hydrophilic nature of the radiotracers. Thus, [^{99m}Tc]TcAMD3465 is expected to behave similarly to the hydrophilic [^{99m}Tc]TcAMD3100 as a suitable agent for tumor imaging without crossing the blood brain barrier (BBB).

In vitro stability study

^{99m}Tc-AMD3465 was found to be stable (> 99% radiochemical purity) in PBS (pH 7.4) and 1% BSA for 24 h at room temperature, similar to [^{99m}Tc]TcAMD3100. It is believed that the stabilization of ^{99m}Tc in AMD3100 and AMD3465 is attributed to the common cyclam structure. The stability was sufficient to further biodistribution and imaging studies.

In vitro receptor binding assays

Jurkat-T cell line expresses high level of CXCR4 and was used in a homologous binding assay to determine the affinity of [^{99m}Tc]TcAMD3465 to CXCR4 receptor. The results are shown in Fig. 2. The IC_{50} value of [^{99m}Tc]TcAMD3465 was 72.2 ± 1.4 μM, indicating a higher affinity than that of [^{99m}Tc]TcAMD3100 (97 ± 3.4 μM) (results not shown). In the literature, Hartimath S.V reported IC_{50} of 92 ± 5 μM for [^{99m}Tc]TcAMD3100 [13].

Biodistribution studies

The biodistribution of [^{99m}Tc]TcAMD3465 in normal NH mice was evaluated at 30, 60 min after injection (Fig. 3). In general, immune tissues such as the blood, kidney, bone, spleen, and liver showed relative high levels of radioactivity at all time points. The accumulation of radioactivity in heart, muscle, lung, and stomach were relatively low. Very low levels of radioactivity were demonstrated in brain, confirming to the anticipated low BBB penetration of [^{99m}Tc]TcAMD3465 due to its high hydrophilicity.

SPECT imaging

SPECT image obtained in normal NH mice 60 min after injection of [^{99m}Tc]TcAMD3465 is shown in Fig. 4a. [^{99m}Tc]TcAMD3465 was excreted from kidneys and bladder. Liver and femur uptake of the tracer was detectably high. No accumulation of radioactivity was observed in healthy brain,

because of the existence of an intact blood-brain barrier and the high hydrophilicity of the radio agent.

A plane projection image from SPECT at 60 min of a mouse bearing a H460 tumor on the right front leg after intravenous injection of 15 MBq [^{99m}Tc]TcAMD3465 is shown in Fig. 4b. The tumor was clearly visible and showed high contrast to the contralateral muscles. The results were consistent with the known overexpression of CXCR4 in H460 cells [21]. High uptake was also seen in the liver, consistent with the biodistribution results of the present study as well as that for [^{64}Cu]CuAMD3465, which was evaluated as a PET tracer for CXCR4 imaging and showed significant accumulation in the liver.

Discussion

The chelation properties of cyclam-based small molecule CXCR4 antagonists, such as AMD3100 and AMD3465, have been utilized for the preparation of radiopharmaceuticals as imaging agents that can be used for diagnosis and post-treatment monitoring of CXCR4 positive tumors. While AMD3100 is approved for stem cell mobilization in patients with lymphoma and multiple myeloma, and the preparation and evaluation of AMD3100 radiolabeled with ^{64}Cu, ^{67}Ga and ^{99m}Tc have been reported, a more potent and selective radioimaging agent that can provide improved specificity and sensitivity is in need. In this regard, AMD3465, a monocyclam structure agent, represents a propelling candidate due to its superior affinity to CXCR4 compared to AMD3100. In the present study, the preparation of [^{99m}Tc]TcAMD3465 using previously optimized procedures for AMD-3100, provided high purity radiocompounds suitable for in vitro and in vivo characterization without further purification. It appears that the pyridyl methylamine group in AMD3465 exerted similar hydrophilicity to the cyclam moiety and the measured logP of [^{99m}Tc]TcAMD3465 was nearly identical to that of [^{99m}Tc]TcAMD3100 and [^{64}Cu]Cu-AMD3465 [19], but more lower than N-[^{11}C]methyl-AMD3465 [20].

The in vitro stability of [^{99m}Tc]TcAMD3465 was evaluated in pH 7.4 buffer and 1% BSA, and no detectable dissociation of technetium from the complex was observed on

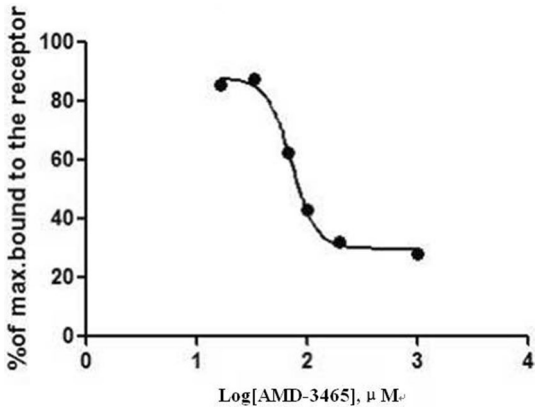

Fig. 2 In vitro homologous AMD3465 displacement assay with [^{99m}Tc]TcAMD3465

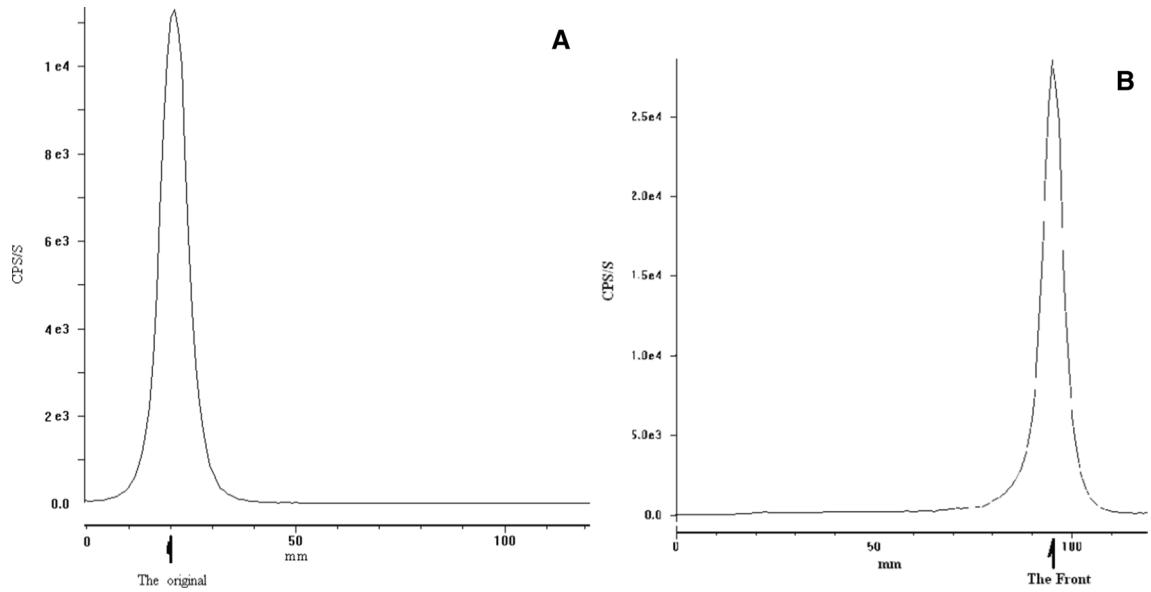

Fig. 1 Radio-TLC chromatograms in **a** acetone, **b** saline

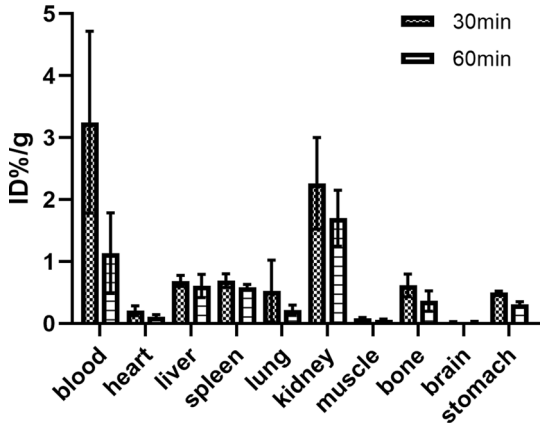

Fig. 3 Biodistribution of [^{99m}Tc]TcAMD3465 in organs of NH mice injected with 3.7 MBq radiotracer

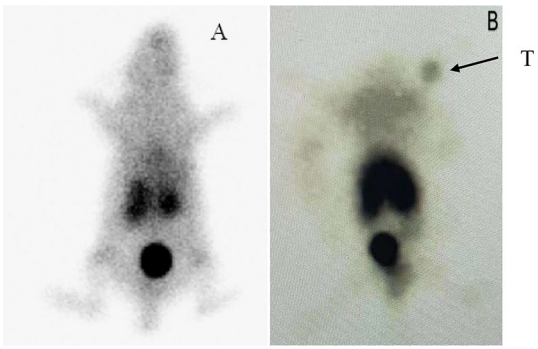

Fig. 4 **a** Normal NH mice imaging with [^{99m}Tc]TcAMD3465; **b** H460 tumor-bearing mice imaging with [^{99m}Tc]TcAMD3465

radio TLC at room temperature for 24 h, suggesting limited metal translocation from the complex to plasma proteins.

As expected, [^{99m}Tc]TcAMD3465 displayed a higher binding affinity for CXCR4 in Jurkat-T cells compare to [^{99m}Tc]TcAMD3100, albeit not as dramatic as metal free ligands. This is likely due to the significant impact of the Tc complexation to the binding affinity of the parent compounds towards CXCR4, which is presumably highly dependent on the interaction between the cyclam and the receptor protein. In the presence of Tc, the availability of protonated tetraaza-functionality of the cyclam for hydrogen bonding or electrostatic interactions with target proteins can diminish dramatically.

The significant uptake of kidney, bone, spleen, and liver is consistent with high expression of CXCR4 in these organs, similar to the biodistribution results observed for [^{99m}Tc]TcAMD3100. However, the accumulation of [^{99m}Tc]TcAMD3465 in liver (< 1%ID/g) was much lower than that of [^{64}Cu]CuAMD3465(40%ID/g) and N-[^{11}C] methyl-AMD3465 [19, 20], .

The SPECT imaging study of [^{99m}Tc]TcAMD3465 was conducted in an H460 lung cancer xenograft mouse model. The clear visualization of the CXCR4 expressing tumor demonstrated potential utility of this new radiotracer, although the significant accumulation of radioactivity in the liver and bladder in both tumor-bearing mice and controls would limit its application in these organs. Also, the in vivo specificity of [^{99m}Tc]TcAMD3465 for CXCR4 remains unclear, and can only be further characterized by additional studies such as blocking experiments and kinetic imaging studies using additional tumor models.

[^{99m}Tc]TcAMD3465 exhibited advantages over [^{64}Cu] CuAMD3465 and N-[^{11}C]methyl-AMD3465. First, the obtention of ^{99m}Tc is easier than ^{64}Cu and ^{11}C, and SPECT imaging is more available and affordable compare to PET/CT. Next, the radiolabeling technology is mature. Last, the physical properties of ^{99m}Tc is favorable, the half-life time of ^{99m}Tc(6 h) is more appropriate for imaging, while longer half-time of ^{64}Cu(13 h) will result more radiation burden to patients and the shorter half-time of ^{11}C(20 min) will limit the use in hospitals without cyclotron. So, for institution without a cyclotron or even without a PET/CT, [^{99m}Tc]TcAMD3465 could be an attractive SPECT tracer for imaging of CXCR4 expression tumors.

Conclusions

AMD3465 was synthesized and successfully labeled with ^{99m}Tc with high labeling yield and good in vitro stability. Homologous CXCR4 binding assays showed IC_{50} value of 72.2 ± 1.4 μM for [^{99m}Tc]TcAMD3465, compared to IC_{50} of 97 ± 3.4 μM for [^{99m}Tc]TcAMD3100. [^{99m}Tc]TcAMD3465 showed high affinity for organs with high CXCR4 expression. In the H460 cell xenograft model, the tumor was clearly visible after injection of [^{99m}Tc]TcAMD3465. The results suggest that [^{99m}Tc]TcAMD3465 could be useful for the imaging of CXCR4 receptor expressing tumors.

Acknowledgements The authors are very grateful to the National Natural Science Foundation of China (81071170) and Beijing Natural Science Foundation (7122162) for financial support.

Author contributions J.Z. and J.T. conceived and designed the experiments; Y.W., X.Z. and Y.G. performed the experiments; Y.W., H.Z. and P.Y. analyzed the data; Z.X. provided reagents/materials/analysis tools; Y.W. wrote the paper.

Compliance with ethical standards

Conflict of interest The authors declare no conflict of interest. The founding sponsors had no role in the design of the study; in the collection, analyses, or interpretation of data; in the writing of the manuscript, and in the decision to publish the results.

References

1. Redjal N, Chan JA, Segal RA, Kung AL (2006) CXCR4 inhibition synergizes with cytotoxic chemotherapy in gliomas. Clin Cancer Res 12:6765–6771
2. Balkwill F (2004) The significance of cancer cell expression of the chemokine receptor CXCR4. Semin Cancer Biol 14:171–179
3. Tanaka T, Bai Z, Srinoulprasert Y, Yang BG, Hayasaka H, Miyasaka M (2005) Chemokines in tumor progression and metastasis. Cancer Sci 96:317–322
4. Kim J, Takeuchi H, Lam ST, Turner RR, Wang HJ, Kuo C, Foshag L, Bilchik AJ, Hoon DS (2005) Chemokine receptor CXCR4 expression in colorectal cancer patients increases the risk for recurrence and for poor survival. J Clin Oncol 23:2744–2753
5. Xiang Z, Zeng Z, Tang Z, Fan J, Zhuang P, Liang Y, Tan YS, He J (2009) Chemokine receptor CXCR4 expression in hepatocellular carcinoma patients increases the risk of bone metastases and poor survival. BMC Cancer 9:176
6. Ling X, Spaeth E, Chen Y, Shi Y, Zhang W, Schober W, Hail N Jr, Konopleva M, Andreeff M (2013) The CXCR4 antagonist AMD3465 regulates oncogenic signaling and invasiveness *in vitro* and prevents breast cancer growth and metastasis *in vivo*. PLoS One 8:e58426
7. Misra P, Lebeche D, Ly H, Schwarzkopf M, Diaz G, Hajjar RJ, Schecter AD, Frangioni JV (2008) Quantitation of CXCR4 expression in myocardial infarction using ^{99m}Tc-labeled SDF-1alpha. J Nucl Med 49:963–969
8. Hanaoka H, Mukai T, Tamamura H, Mori T, Ishino S, Ogawa K, Iida Y, Doi R, Fujii N, Saji H (2006) Development of a ^{111}In-labeled peptide derivative targeting a chemokine receptor, CXCR4, for imaging tumors. Nucl Med Biol 33:489–494
9. Jacobson O, Weiss ID, Kiesewetter DO, Farber JM, Chen X (2010) PET of tumor CXCR4 expression with 4-^{18}F-T140. J Nucl Med 51:1796–1804
10. Boulais PE, Dulude D, Cabana J, Heveker N, Escher E, Lavigne P, Leduc R (2009) Photolabeling identifies transmembrane domain 4 of CXCR4 as a T140 binding site. Biochem Pharmacol 78:1382–1390
11. Lapa C, Lückerath K, Kleinlein I, Monoranu CM, Linsenmann T, Kessler AF, Rudelius M, Kropf S, Buck AK, Ernestus RI, Wester HJ, Löhr M, Herrmann K (2016) ^{68}Ga-pentixafor-PET/CT for imaging of chemokine receptor 4 expression in glioblastoma. Theranostics 6:428–434
12. Zhang JM, Tian JH, Li TR, Guo HY, Shen L (2010) ^{99m}Tc-AMD3100: a novel potential receptor-based target radiopharmaceutical for tumor imaging. Chin Chem Lett 21:461–463
13. Hartimath SV, Domanska UM, Walenkamp AM, Rudi AJOD, de Vries EF (2013) [^{99m}Tc]O2-AMD3100 as a SPECT tracer for CXCR4 receptor imaging. Nucl Med Biol 40:507–517
14. Jacobson O, Weiss ID, Szajek L, Farber JM, Kiesewetter DO (2009) ^{64}Cu-AMD3100—a novel imaging agent for targeting chemokine receptor CXCR4. Bioorg Med Chem 17:1486–1493
15. Nimmagadda S, Pullambhatla M, Stone K, Green G, Bhujwalla ZM, Pomper MG (2010) Molecular imaging of CXCR4 receptor expression in human cancer xenografts with ^{64}Cu-AMD3100 positron emission tomography. Cancer Res 70:3935–3944
16. Aghanejad A, Jalilian AR, Fazaeli Y, Alirezapoor B, Pouladi M, Beiki D, Maus S, Khalaj A (2013) Synthesis and evaluation of ^{67}Ga-AMD3100: a novel imaging agent for targeting the chemokine receptor CXCR4. Sci Pharm 82:29–42
17. Hatse S, Princen K, Declercq E, Rosenkilde MM, Schwartz TW, Hernandez-Abad PE, Skerlj RT, Bridger GJ, Schols D (2005) AMD3465, a monomacrocyclic CXCR4 antagonist and potent HIV entry inhibitor. Biochem Pharmacol 70:752–761
18. Bodart V, Anastassov V, Darkes MC, Idzan SR, Labrecque J, Lau G, Mosi RM, Neff KS, Nelson KL, Ruzek MC, Patel K, Santucci Z, Scarborough R, Wong RS, Bridger GJ, Macfarland RT, Fricker SP (2009) Pharmacology of AMD3465: a small molecule antagonist of the chemokine receptor CXCR4. Biochem Pharmacol 78:993–1000
19. DeSilva RA, Peyre K, Pullambhatla M, Fox JJ, Pomper MG, Nimmagadda S (2011) Imaging CXCR4 expression in human cancer xenografts: evaluation of monocyclam^{64}Cu-AMD3465. J Nucl Med 52:986–993
20. Hartimath SV, Waarde AV, Dierckx RAJO, Vries EFJ (2014) Evaluation of N [11C]Methyl-AMD3465 as a PET tracer for imaging of CXCR4 receptor expression in a C6 glioma tumor model. Mol Pharm 11:3810
21. Liang CY, Liu HF1, Liu X, Zhou NK, Zhang JM, Guo J (2011) Expression of CXCR4 protein and mRNA in different lung cancer cell lines. J Chin PLA Postgrad Med Sch 32:757–759
22. Gui Y, Xu ZH, Zhang XJ, Zhang SW, Liu J, Tian JH, Zhang JM (2013) Synthesis of AMD3100 for antagonist of CXCR4 and labeled with ^{99m}Tc. Isotopes 26:158–162